PHILOSOPHICAL TRANSACTIONS OF THE ROYAL SOCIETY A MATHEMATICAL, PHYSICAL & ENGINEERING SCIENCES

On Spikes and Spots: Strongly Nonlinear Theory and Experimental Comparisons

F. T. Smith

Phil. Trans. R. Soc. Lond. A 1995 **352**, 405-424
doi: 10.1098/rsta.1995.0079

On spikes and spots: strongly nonlinear theory and experimental comparisons

By F. T. Smith

Mathematics Department, University College, Gower Street, London WC1E 6BT, UK

Spikes and spots are discussed mostly for incompressible boundary layers, with the emphasis towards strong nonlinearity. The distinction between forced and free disturbances then becomes blurred, as spikes and spots reproduce each other. First, the forced case is concentrated on the start of spikes. The theory used is that of the two- or three-dimensional interacting boundary layer, capturing nonlinear Tollmien–Schlichting waves, for example, or following a vortex-wave interaction. Finite-time breakup produces shortened time and length scales, yielding agreement with computations and experiments on the first spike in transition, with subsequent spot formation. After the breakup, normal pressure gradients and vortex wind-up become significant locally. Second, the free case concerns initial-value problems for spots containing a wide band of three-dimensional nonlinear disturbances. The theory points to successive nonlinear stages starting at the wing tips near the spot trailing edge but gradually entering the middle as the amplitudes increase downstream. This effect combined with shortening scales produces a spread angle near 11°, very close to the experimental observations. The overall spot structure is described briefly, including also the leading edge. Viscosity arises later in two ways; for the case mentioned above with spikes originating near the surface and also through a novel interaction influencing the global spot.

1. Introduction

This research on spikes, spots and their reproductions is directed toward greater theoretical understanding of deep transition and, ultimately, turbulent flow and turbulence modelling if possible. The theoretical understanding, for example, of scales, should help to guide direct computational simulations, as well as providing parametrization and comparisons with experiments. Here, for the incompressible regime mostly, we highlight certain central points of the three main nonlinear theories involved, i.e. (A) vortex/wave interaction theory, (B) pressure-displacement interactive boundary-layer theory and (C) high-frequency cum Euler-scale theory, corresponding basically to increasing amplitudes in turn. This is as opposed to providing a broad review of what is now a vast research area and would require enormous journal space. Theories (A)–(C) are described within §2 and 3, specifically (B) in §2, (C) in §3, but with elements of (A) in both sections. We address not only the slower types of transition but also the bypass types, referred to later on. Moreover, attention is drawn to nonlinear interactions which completely alter the mean-flow profiles, and that means the preceding three. Their major assumption is that the

Phil. Trans. R. Soc. Lond. A (1995) **352**, 405–424
Printed in Great Britain

typical global Reynolds number Re is large, which seems in line with the practical interest in large Re values.

Concerning *forced* disturbances first, many kinds of boundary-layer transition are observed in practice, depending on the disturbance environment, e.g. with surface roughness or freestream unsteadiness. One extreme path is the 'fast' bypass transition epitomized by pipe-flow transition and by the wake-passing effect, from an upstream row of rotor blades, on the boundary layers on stator blades in turbines. The other possible extreme is a 'slow' transition path, starting from linear Tollmien–Schlichting (TS) instability. This is exemplified by extensions of the classical experiments by Schubauer and Skramstad in the 1940s (see, for example, Stuart 1963) on tiny unsteady controlled disturbances introduced upstream into a basic planar laminar boundary layer. The typical progression here is linear two-dimensional decay, then growth, then nonlinear three-dimensional motion. For sufficiently large (although still small) amplitudes, significant three-dimensional action can appear downstream with a preferred cross-stream wave number or a sustained vortex-like pattern of quite long streamwise length scale. Alternatively, there is the classic transition path of Klebanoff & Tidstrom (1959), Nishioka *et al.* (1979). There, nearly planar input disturbances upstream lead on within a relatively short distance to the formation of strongly three-dimensional streets downstream, in which turbulent bursts or spots are initiated; later we describe theoretical–experimental comparisons for this path. In addition, intermittency may occur in any of the preceding stages experimentally, depending on the disturbance environment. Turbulent flow ensues some way downstream, but the nominally full turbulent state eventually reached may be regarded as broadly the same as that reached via the fast type of bypass transition described earlier.

Section 2 below on spikes, for example in initially forced transition, considers nonlinear theory (B) for nonlinear TS or interacting-boundary-layer (IBL) interactions, which are controlled by the unsteady IBL equations. Emphasis is given to the recent findings of nonlinear finite-time breakups (Smith 1988*a*; Peridier *et al.* 1991*a*, *b*; Hoyle *et al.* 1991), detailed comparisons with computations and experiments, and the repercussions. This breakup refers to a singularity that is encountered in the IBL system, in general, within a finite scaled time and involves the scaled pressure gradient and skin friction, among other properties, becoming unbounded locally. A local change of scales is therefore induced. The repercussions of this are concerned principally with local sublayer eruption and vortex formation.

Second, concerning *free* disturbances, the three-dimensional 'spot' or travelling disturbance results from an initial localized disturbance and exhibits downstream travel, some amplitude growth and spatial spreading of the spot. Three basic types may be identified, namely laminar, transitional and turbulent spots, depending on the amplitude and spectra of the initial disturbance. All three are of much interest in terms of fundamental fluid dynamics and applications. Numerous aspects of turbulent spots have been studied experimentally, with fascinating and somewhat varied results, for example on the main arrowhead-shaped part of the spot, its tail, its notional speed, and its spreading rate. See contributions stretching from Emmons (1951), Schubauer & Klebanoff (1956), Lighthill (1963), Schlichting (1979), Falco (1979) to Head & Bandyopadhyay (1981), Perry *et al.* 1981, Chambers & Thomas (1983), Smith *et al.* (1991), Gad-el-Hak *et al.* (1981), Katz *et al.* (1990), Johansson *et al.* (1987), Henningson & Alfredson (1987) and Robinson (1991). Outstanding features found experimentally include the following. Much of the dynamics

PHILOSOPHICAL TRANSACTIONS OF THE ROYAL SOCIETY A MATHEMATICAL, PHYSICAL & ENGINEERING SCIENCES

in a spot closely resembles that in a fully turbulent boundary layer; a turbulent spot develops fast, typically from localized disturbances with large initial amplitude; the subsequent growth and spreading of a fully turbulent spot probably take place in a domino-like manner, possibly associated with the successive production of hairpin vortices in the flow near the solid surface; the spanwise growth of the spot greatly exceeds the growth normal to the surface; and the leading edge and the spanwise side edges are notably sharp, with interaction between the spot and trailing waves packets especially near the sides. Several other experimental features are also described in the above papers. Again, interesting computations have been performed on transitional/turbulent spots, mostly for channel flows and more recently for boundary layers. Most are confined to spatially periodic boundary conditions but, for a large period, they seem to reproduce fairly well some of the major experimental findings. Examples are in Leonard (1981), Bullister & Orszag (1987), Henningson *et al.* (1987), Henningson & Kim (1991), Lundbladh & Johansson (1991), Fasel (1990), Konzelmann & Fasel (1991). Much extra physical insight and understanding have still to be provided, nevertheless. Systematic tracking of the effects of increasing amplitude, for instance, largely remains to be done, both experimentally and computationally.

Few, if any, systematic theoretical studies had been made either, until recently, especially on the scales and flow structures necessary for a clear physical understanding of the spot's behaviour. A strongly nonlinear theory is desirable, and the research below appears to be the only effort in that direction, specifically for spot evolution, i.e. the initial-value problem. Our prime aim here, combined with the related works (Doorly & Smith 1992; Smith 1991*a*, 1992; Smith *et al.* 1994; see also Gaster 1968), is to consider recent nonlinear theory and address the experimental findings above. Much of these findings can be described by the theory, even though many complex phenomena arise during spot evolution. In practice, there is significant dependence on the particular experimental configurations and conditions used, and there are many nonlinear aspects still to be explained or explored. The Euler stage (theory C) of Smith *et al.* (1990), Smith & Burggraf (1985) (and see also Zhuk & Ryzhov 1982) appears to be the closest, of any rational theory for high Re, to describing boundary-layer turbulence in a systematic fashion. Support is given in the above papers and also by the more empirical modelling of Walker (1990) (see also Smith *et al.* 1991; Hoyle *et al.* 1991; Peridier *et al.* 1991*a*, *b*). This Euler stage corresponds to nonlinear disturbance wavenumbers α, β, frequencies ω, propagation speeds c and amplitudes (for example, pressure p', velocity $\boldsymbol{u}'$) all of $O(1)$, based on the boundary-layer thickness and local freestream speed, thus representing a wider range than conventional linear-type TS disturbances, which have α, β, ω, c, $|p'|$, $|\boldsymbol{u}'|$ all smaller by an order of magnitude. In consequence, it seems not unreasonable to tackle the free spot-evolution problem theoretically first by means of the same Euler-stage nonlinear approach, but as a nonlinear 3D initial-value problem for a localized input disturbance (rather than a fixed-frequency problem, for example). This is the concern of much of § 3.

Section 3 (*a*)–(*e*) tends to split the *spot* dynamics into two categories, global (mainly inviscid) and internal (viscous-inviscid) properties, and to concentrate on the former. Nevertheless, a new long/short-scale global interaction is identified in § 3 *d*, linking the 3D viscous boundary-layer equations and unsteady Euler equations via Reynolds-stress forces, sufficiently far downstream. Moreover, internal properties, flow structures and their interactions with the more global dynamics are reconsidered briefly in § 3 *e*, having been addressed in more detail in § 2. The viscous sublayer, its

PHILOSOPHICAL TRANSACTIONS OF THE ROYAL SOCIETY A MATHEMATICAL, PHYSICAL & ENGINEERING SCIENCES

eruptions and the ensuing local vortex formations can become important in practice. Not least, they introduce shorter length and time scales, and hence even higher frequency and wavenumber content, and they almost certainly play a key part in the domino process mentioned earlier. The work is aimed at relatively high-amplitude nonlinear responses, as opposed to gradual transition following linear instability. The latter transition for spots is considered in Cohen *et al.*'s (1991) interesting, mainly experimental, study, i.e. with input spectrum corresponding essentially to longer TS length and time scales, lower amplitudes and relatively slow propagation (until breakdown occurs later on), in contrast with the present *wider* spectrum of faster Euler scales, high amplitudes and faster propagation, equivalent to a nonlinear bypass mechanism. Many issues are left unresolved, and research into some of these is in progress. The major physical effects investigated in § 3 are through nonlinear interactions between the fluctuations present and the mean flow. Further comments are provided in § 4, including the inter-relations between spikes and spots and further questions.

2. IBL transitions and breakup: spikes

The velocities $(\overline{u}, \overline{v}, \overline{w})$ in Cartesian coordinates $(\overline{x}, \overline{y}, \overline{z})$ (streamwise, normal, spanwise), the pressure $\overline{p}$ and the time $\overline{t}$ are assumed to be non-dimensionalized globally, with respect to (say) airfoil chord and freestream speed. Given that Re is a large parameter, we address the Navier–Stokes equations but scale the variables here in the TS lower-branch fashion (Smith 1979*a*, *b*). That is equivalent to the triple-deck scalings

$$(\overline{u}, \overline{v}, \overline{w}) = (Re^{-1/8}\,\lambda^{1/4}u, Re^{-3/8}\,\lambda^{3/4}v, Re^{-1/8}\,\lambda^{1/4}w) + \cdots, \tag{2.1}$$

$$\overline{p} = Re^{-1/4}\,\lambda^{1/2}p(X, Z, T) + \cdots, \tag{2.2}$$

$$(\overline{x}, \overline{y}, \overline{z}, \overline{t}) = (\overline{x}_0 + Re^{-3/8}\,\lambda^{-5/4}X, Re^{-5/8}\,\lambda^{-3/4}Y, \overline{z}_0 + Re^{-3/8}\,\lambda^{-5/4}Z, Re^{-1/4}\,\lambda^{-3/2}T). \tag{2.3}$$

The scalings apply in the so-called lower deck, which is a viscous sublayer close to the surface. The factor $\lambda = \lambda(\overline{x}_0, \overline{z}_0)$ is the reduced skin friction of the oncoming undisturbed $O(Re^{-1/2})$ thick boundary layer, e.g. in Blasius flow $\lambda \propto {\overline{x}_0}^{-1/2}$, at the typical $O(1)$ station $\overline{x} = \overline{x}_0, \overline{z} = \overline{z}_0$. The flow problem comes down to the unsteady nonlinear IBL problem:

$$\frac{\partial u}{\partial X} + \frac{\partial v}{\partial Y} + \frac{\partial w}{\partial Z} = 0, \tag{2.4}$$

$$\left(\frac{\partial}{\partial T} + u\frac{\partial}{\partial X} + v\frac{\partial}{\partial Y} + w\frac{\partial}{\partial Z}\right)(u, w) = -\left(\frac{\partial p}{\partial X}, \frac{\partial p}{\partial Z}\right) + \frac{\partial^2 (u, w)}{\partial Y^2}, \tag{2.5}$$

$$u = v = w = 0, \quad \text{at } Y = 0 \text{ (no slip)}, \tag{2.6}$$

$$u \sim Y + A(X, Z, T), \quad w \to 0 \text{ as } Y \to \infty \text{ (unknown displacement)}, \tag{2.7}$$

$$p(X, Z, T) = -\frac{1}{2\pi}\int_{-\infty}^{\infty}\int_{-\infty}^{\infty} \frac{\partial^2 A/\partial\chi^2(\chi, \phi, T)\,\mathrm{d}\chi\,\mathrm{d}\phi}{[(X-\chi)^2 + (Z-\phi)^2]^{1/2}} \text{ (interaction law)}. \tag{2.8}$$

Here (2.8) applies for subsonic flow. In the 2D supersonic counterpart, (2.8) is replaced by Ackeret's law $p = -\partial A/\partial X$. There are, in addition, finite Re versions of much interest. The two main alternatives to the nonlinear triple-deck version above

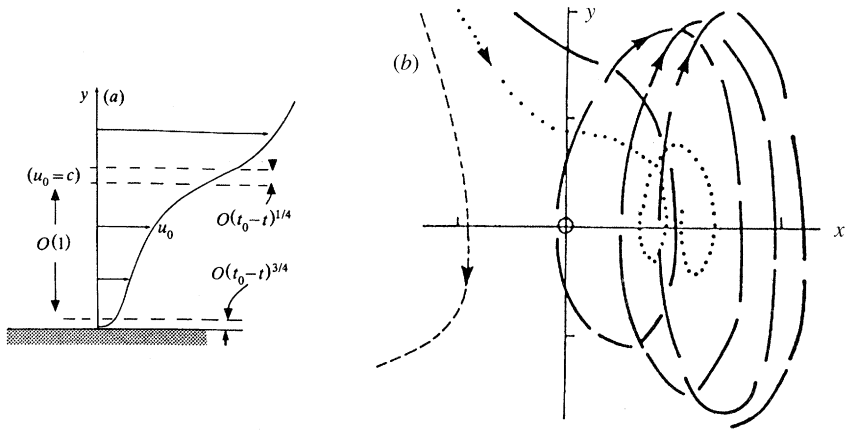

Figure 1. (*a*) Finite-time breakup structure (§ 2) in 2D or 3D: typical velocity profile with the main Y scale of $O(1)$ and subsidiary scales, while Z is given by (2.14). (*b*) Computed 2D solutions for the particle trajectories during subsequent vortex formation and roll-up.

are the Navier–Stokes equations and IBL and related versions at finite Re. Both require numerical treatments. In general, the former tends to be hindered more by grid-resolution difficulties, among others. IBL and similar methods, which are more zonal treatments involving sensible interpretations of (2.4)–(2.8) at finite Re, have been developed only fairly recently for unsteady flows (Smith *et al.* 1984; Peridier *et al.* 1991*b*). These have connections with interesting methods based on the parabolized Navier–Stokes equations (Bertolotti *et al.* (1992) and independent work by Dr M. R. Malik), which have also been developed recently.

Some properties of the viscous-inviscid unsteady nonlinear system (2.4)–(2.8) and related problems are well known (see, for example, Smith 1979*b*; Hall & Smith 1984; Smith & Burggraf 1985). The linearized version, linearized about the original steady flow $u = Y$, $v = w = p = A = 0$, compares well with Orr–Sommerfeld results in two dimensions. It gives the neutral scaled frequency $\Omega = \Omega_{\rm n} \approx 2.30$, where $\partial/\partial T \rightarrow -{\rm i}\Omega$. A supercritical 2D bifurcation is present for $\Omega > \Omega_{\rm n}$, which is equivalent to $x_0 > x_{0{\rm n}}$ or a displacement-thickness Reynolds number $Re_\delta > Re_{\delta n}$, in view of the λ factor, cf. Hall & Smith (1984) in three dimensions. Computations of nonlinear travelling states for a range of values of Ω greater than $\Omega_{\rm n}$ have been presented by Conlisk *et al.* (1987), since which more have been done. These are connected at increasing frequency with § 3 and with the reversed-flow singularities discussed in Smith (1988*b*). Again, there are applications to linear receptivity in Goldstein (1985), Goldstein & Hultgren (1989), Ruban (1985) and to nonlinear receptivity in Smith (1987). Even with continued forcing, for example, at almost fixed frequency as with a vibrating ribbon experiment, however, the time evolution is important especially with regard to the occurrence of singularities, cf. Smith (1988*b*) in the fixed-frequency case. Relatively early numerical results for time-marching are presented by Duck (1985), Smith (1984), whereas more recent accurate computations are given by Peridier *et al.* (1991*a*, *b*).

Most recent interest is in the ultimate behaviour of the nonlinear time-marching regime, where, for finite amplitudes, the unsteady IBL system (2.4)–(2.8) applies in full. The principal finding seems to be that localized finite-time breakups can occur (Smith 1988*a*): see figure 1. These breakups take the form, in two dimensions,

$$X - X_{\rm s} = c(T - T_{\rm s}) + (T_{\rm s} - T)^N \xi,$$

Table 1. *Values of the power $\widetilde{B}$ at various Re values*

	$\widetilde{B}$ (from computations)	$\widetilde{B}$ (from theory)
Re	Peridier *et al.* (1991*b*)	Smith (1988*a*)
10^8	-0.252 ± 0.016	-0.25
10^7	-0.253 ± 0.035	-0.25
10^6	-0.263 ± 0.022	-0.25
10^5	-0.234 ± 0.032	-0.25

$$\frac{\partial p}{\partial X} \sim (T_s - T)^{-1} p_1'(\xi), \quad u \to u_0(Y) \tag{2.9}$$

near the breakup position X_s and time T_s. Here the local velocity profile u_0 is smooth, with $u_0 = c$ at the inflection point, the local coordinate ξ is of $O(1)$, and the phase speed c is of $O(1)$. It is found that the power $N = \frac{3}{2}, \frac{5}{4}, \frac{7}{6}, \frac{9}{8}, \ldots, 1$ for single-valuedness. In moderate breakups, $N > 1$. Then, in effect, an inviscid Burgers equation for the pressure function $p_1(\xi)$ describes the local terminal behaviour

$$p_1 p_1' = b_1(p_1 - 3\xi p_1') \tag{2.10}$$

in scaled terms, from substitution into (2.4)–(2.8) and integration with respect to Y. (2.10) is for the most likely case of $N = \frac{3}{2}$ and holds provided the integral constraint (ref2.13) on u_0 is satisfied. This yields the appropriate smooth solution

$$\xi = -b_2 p_1 - b_3 p_1^3 \tag{2.11}$$

implicitly, where b_2 and b_3 are constants having the same sign. (2.11) shows that the $p_1(\xi)$ solution is single valued as required and monotonic in ξ. Furthermore, $|p_1| \propto |\xi|^{1/3}$ at large $|\xi|$. This asymptote matches with the flow solution further away from the breakup station $X = X_s$ and gives specifically the behaviour

$$p - p_0 \propto |X - X_s|^{1/3}, \quad \text{as } X \to X_s\pm, \tag{2.12}$$

where $p_0 \equiv p(X_s)$ is a constant. Hence, a singularity in the pressure gradient is predicted at the breakup time $T = T_s$. For $N = 1$, on the other hand, we have severe breakups, see last reference. Both sorts of breakup provoke increasingly large wall-shear responses in the local motion. Various previous unsteady IBL computations appear to support qualitatively the singular description in (2.9)–(2.12). There is also fair agreement with the Navier–Stokes computations of Fasel (1984), whereas experimental comparisons are described nearer the end of this section. A significant point is that the breakup applies to most of the unsteady interactive flows known to date.

Detailed quantitative comparisons between computations of (2.4)–(2.8) and the breakup theory of (2.9)–(2.12), for $N = \frac{3}{2}$, are made by Peridier *et al.* (1991*b*), showing very good agreement; see also figure 1. Table 1 compares (at various *Re* values) the values of the power $\widetilde{B}$ implied by the numerical results in Peridier *et al.* (1991*b*) with the value $\widetilde{B} = -\frac{1}{4}$ implied by the theory above. The agreement is felt to be encouraging. The power here occurs in the behaviour $\tau_w \propto (T_s - T)^B$ of the scaled skin friction.

Following the breakup, new physical effects come into play locally as normal pressure gradients become significant on shorter length scales. An appropriate computational approach, in principle, can then be found in Smith *et al.* (1984), Smith (1991*b*).

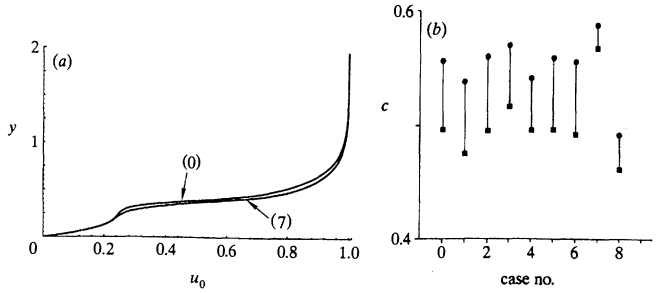

Figure 2. Comparisons between theory (Smith & Bowles 1992) and experiment (Nishioka *et al.* 1979), concerning the nonlinear criterion (2.13) and the first transitional spike. All the cases (0)–(8) studied are close to the two representative cases (0), (7) for the local experimental profile shown in (*a*). In (*b*), the circles effectively denote theoretical results and the squares experimental results. Note that the complete range of possible c values is between 0 and 1, and that the variation with case number in (*b*) indicates sensitivity with respect to the velocity-profile measurement.

The new faster stage is discussed by Hoyle *et al.* (1991) where it is shown that an extended KdV equation holds for the pressure, subject to matching at large negative scaled times with the breakup of (2.9)–(2.12). Beyond that, another new stage of still faster time scales is encountered as a strong local vortex formation takes place (figure 1 and Bowles *et al.* 1995). This is felt to be associated with the initiation and eruption of a vortex in the viscous layer. Intuition would suggest also that this breakup process, when repeated, may well be connected with the occurrence of intermittency in practice. Smith and Bowles (1992) make comparisons, as shown in figure 2, between the breakup criterion (Smith 1988*a*) that arises from (2.9)–(2.12), namely

$$\int_0^\infty [u_0(Y) - c]^{-2}\,\mathrm{d}Y = 0, \tag{2.13}$$

and the experimental measurements of Nishioka *et al.* (1979) concerning *the first spike* in transition. The agreement found is relatively close, especially given that Re is subcritical in the experiments.

There are many related or follow-on aspects. First, high-frequency theory applied to (2.4)–(2.8) yields an alternative view of spikes, associated more with still larger disturbances, as discussed in § 3 *e* below. In the same regime, Kachanov *et al.* (1993) compare 2D nonlinear theory and experiments showing other apparent spikes, finding good agreement as shown in figure 3; while at suitably reduced amplitudes, upper-branch features and critical layers tend to arise further downstream of the lower-branch regime (2.1)–(2.8). Second, there is recent work by Vickers & Smith (1994) on the breakup of separating flows (see also Savenkov 1993). Next, Hoyle & Smith (1994) consider the extension of (2.9)–(2.13) to three dimensions, where

$$Z - Z_\mathrm{s} \sim (T_\mathrm{s} - T)^{5/4}. \tag{2.14}$$

gives a crucial spanwise scale when $N = \frac{3}{2}$ in (2.9). Likewise, in three dimensions, Smith & Walton (1989), Stewart & Smith (1992) and Smith & Bowles (1992) imply that vortex/wave interactions (theory A in § 1) based on (2.4)–(2.8), for example, can act at low input amplitudes as precursors to the strong-amplitude finite-time breakup above. The latter two yield good agreement with boundary-layer and channel flow experiments (figures 4, 5), in addition to that above. Other vortex/wave interactions are studied in the series by Hall & Smith (1988, 1989, 1990, 1991), with

PHILOSOPHICAL TRANSACTIONS OF THE ROYAL SOCIETY A MATHEMATICAL, PHYSICAL & ENGINEERING SCIENCES

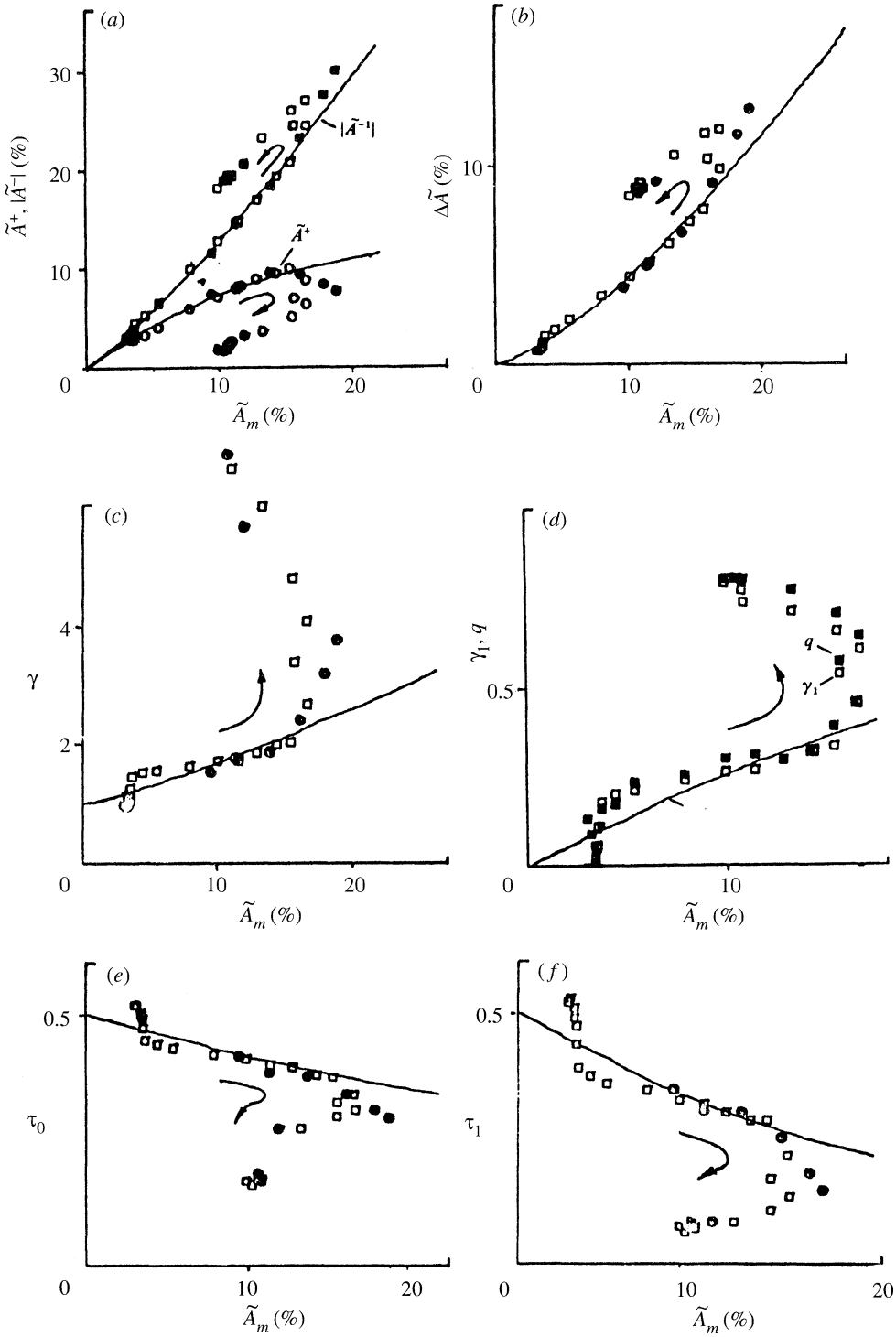

Figure 3. A comparison with experimental work in Kachanov *et al.* (1993), in mostly quasi-2D transition.

PHILOSOPHICAL TRANSACTIONS OF THE ROYAL SOCIETY A MATHEMATICAL, PHYSICAL & ENGINEERING SCIENCES

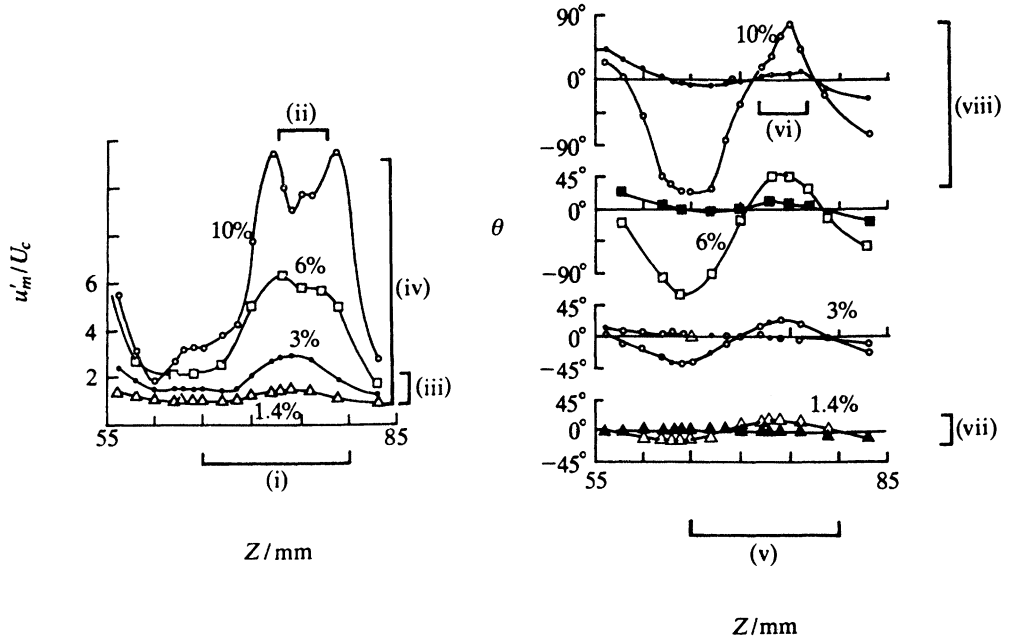

Figure 4. A comparison with experimental work, from Smith & Bowles (1992), in the channel-flow 3D transition of Nishioka *et al.* (1979). Theoretical results are shown as bars (i)–(viii).

related works by Benney & Chow (1989), Wu (1993), Churilov & Shukhman (1987, 1988), Walton & Smith (1992), Timoshin & Smith (1995), Walton *et al.* (1994) and Smith *et al.* (1993), in various weakly or strongly nonlinear settings with TS or inflectional disturbances. Hall & Smith (1988, 1989, 1990, 1991), in particular, emphasize the ability of vortex–wave interactions to provoke strongly nonlinear effects even for quite tiny 3D input disturbances. Vortex effects are clearly very powerful, both theoretically and in practice. Finally here, further work, following on directly from (2.9)–(2.13), is mentioned later.

3. The free evolving spot

The focus shifts now to the evolution of free spots, corresponding to nonlinear initial-value problems including shorter scales, cf. the forced spots arising in § 2. The main context here concerns the Euler stage for large fully nonlinear disturbances, where the unsteady nonlinear 3D incompressible Euler equations apply throughout the boundary layer:

$$\overline{u}_x + \overline{v}_y + \overline{w}_z = 0, \tag{3.1}$$

$$\overline{u}_t + \overline{u}\,\overline{u}_x + \overline{v}\,\overline{u}_y + \overline{w}\,\overline{u}_z = -\overline{p}_x, \tag{3.2}$$

$$\overline{v}_t + \overline{u}\,\overline{v}_x + \overline{v}\,\overline{u}_y + \overline{w}\,\overline{v}_z = -\overline{p}_y, \tag{3.3}$$

$$\overline{w}_t + \overline{u}\,\overline{w}_x + \overline{u}\,\overline{w}_y + \overline{w}\,\overline{w}_z = -\overline{p}_z. \tag{3.4}$$

The coordinates, with an origin shift, are scaled on the typical boundary-layer thickness $O(Re^{-1/2})$, and similarly for the $O(Re^{-1/2})$ timescale t. The main boundary conditions are

$$(\overline{u}, \overline{v}, \overline{w}, \overline{p}) \to (u_e, 0, w_e, 0), \quad \text{as } y \to \infty, \tag{3.5}$$

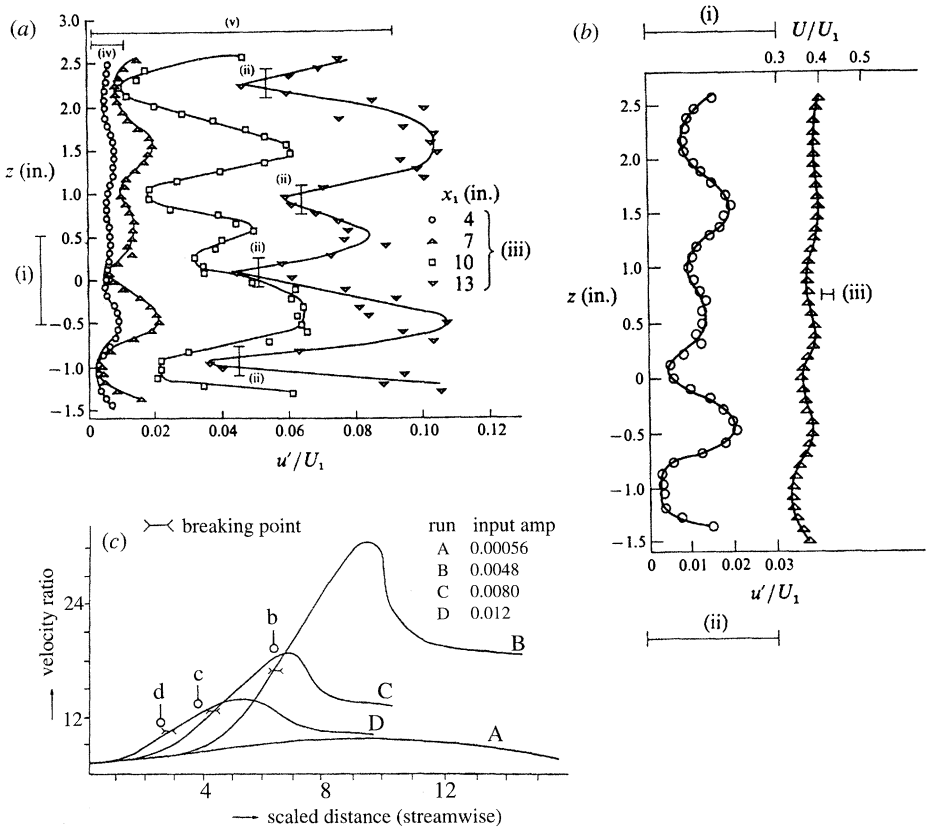

Figure 5. A comparison with Stewart & Smith (1992), in the boundary-layer 3D transition of Klebanoff & Tidstrom (1959). Theoretical predictions are indicated by bars (i)–(v) in (*a*), (i)–(iii) in (*b*), and b, c, d (compared with experimental breaking points) in (*c*).

$$(\overline{u},\overline{v},\overline{w},\overline{p}) \to (u_{\mathrm{B}}(y),0,w_{\mathrm{B}}(y),0), \quad \text{as } x^2+z^2 \to \infty, \tag{3.6}$$

$$\overline{v}=0 \text{ at } y=0. \tag{3.7}$$

The conditions (3.5) and (3.6) are to match with the free stream outside the boundary layer and with the undisturbed boundary-layer profile $u_{\mathrm{B}}(y)$ holding sufficiently far from the initial disturbance, and (3.7) is the tangential-flow constraint at the solid surface. For the present $u_{\mathrm{e}} \equiv 1$, $w_{\mathrm{e}} = w_{\mathrm{B}}(y) \equiv 0$, but compare §3*d* below. The profile $u_{\mathrm{B}}(y)$ here is supposed to be monotonic, inflection-free, and $u_{\mathrm{B}}(\infty) = 1$, $u'_{\mathrm{B}}(0) = \lambda_{\mathrm{B}} > 0$. The initial disturbance itself is fully nonlinear in general, so that $(\overline{u},\overline{v},\overline{w},\overline{p})$ is prescribed for all x, y, z at $t = 0$, consistent with (3.1)–(3.4). The problem (3.1)–(3.7) is usually a computational one.

The work in Smith *et al.* (1992, 1994) considers the possible solution properties of the nonlinear initial-value problem above at large times, and especially far downstream of the initial-disturbance position, given guidance from the linearized analysis of Doorly & Smith (1992). At large times t, two major length scales arise in the plan view (x–z plane): one very far downstream at distances $O(t)$ and the other less far downstream, at distances $O(t^{1/2})$. Below we are concerned first with the $O(t^{1/2})$ length scale, since significant features are found to arise there first, even though this zone trails the majority (the $O(t)$ zone, see (*d*)) of the spot (see figure 6). An order-of-magnitude argument suggests the perhaps surprising feature that, in the $O(t^{1/2})$

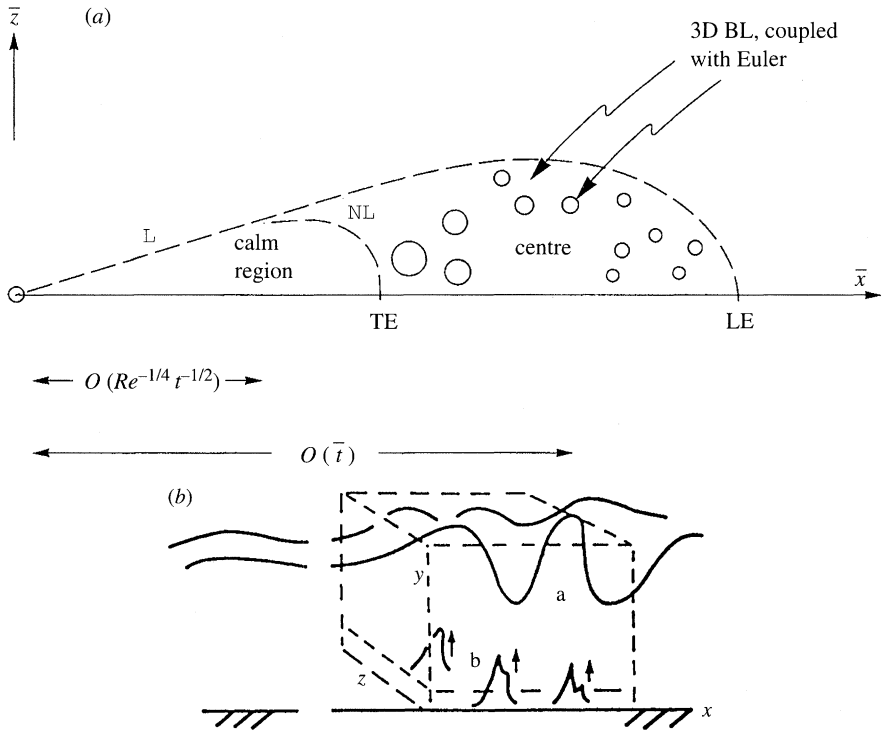

Figure 6. (a) Plan view of the theoretical spot structure in § 3, with symmetry about the $\overline{x}$-axis. In § 3 *a–c* $Re^{-1/2} \ll \bar{t} \ll 1$, whereas when time $\bar{t}$ becomes $O(1)$, in § 3 *d*,*e*, coupling occurs between the global (3DBL) and local (Euler, see (*b*)) properties as indicated. $\mathcal{L}, \mathcal{NL}$ denote linear and nonlinear regions in turn, the former envisaged as bounding the calm region observed in experiments, while LE, TE denote the leading and trailing edges respectively. (*b*) The local 3D Euler structure a and subsequent sublayer eruptions b, leading to spots within spots: see § 2, § 3 *e*.

zone, the large-time solution of the unsteady Euler problem takes on a three-layer form, analogous with the triple-deck structure. The 'lowest' layer has y being small with

$$(\overline{u}, \overline{v}, \overline{w}, \overline{p}) \sim [t^{-1}U, t^{-3/2}V, t^{-1/2}W, t^{-1}P], \quad y = t^{-1/2}\overline{Y}, \tag{3.8}$$

whereas in the 'middle' layer

$$(\overline{u}, \overline{v}, \overline{w}, \overline{p}) \sim [u_{\mathrm{B}}(y) + t^{1/2}Au'_{\mathrm{B}}, -t^{-1}A_{\overline{X}}u_{\mathrm{B}}(y), O(t^{-1}), t^{-1}P], \quad y = O(1), \tag{3.9}$$

and in the 'uppermost' layer in the outer reaches of the boundary layer

$$(\overline{u}, \overline{v}, \overline{w}, \overline{p}) \sim [1 + t^{-1}\overline{u}_1, t^{-1}\overline{v}_1, t^{-1}\overline{w}_1, t^{-1}\overline{p}], \quad y = O(t^{1/2}). \tag{3.10}$$

Here the unknown surface pressure $P(\overline{X}, \overline{Z})$ and negative displacement $A(\overline{X}, \overline{Z})$ depend on the scaled coordinates $(\overline{X}, \overline{Z})$ defined by

$$(x, z) = t^{1/2}(\overline{X}, \overline{Z}) \tag{3.11}$$

in the present zone. From substitution into (3.1)–(3.7) we are left with solving a nonlinear similarity inviscid-boundary-layer-like system for the $O(t^{1/2})$ zone properties. The theory and allied computations in § 3 *a–c* below are concerned mostly with the 'trailing edge' of the spot, where the coordinates $(\overline{X}, \overline{Z})$ are typically large and

positive, between the $O(t^{1/2})$ and $O(t)$ zones downstream, with the latter then being discussed in § 3 *d*,*e*. The lowest level of input or evolved amplitude that produces a significant nonlinear response in the spot trailing edge is considered first.

(*a*) *Amplitude level I*

The flow solution at comparatively large distances $\overline{X} \gg 1$ downstream in the edge layer near $\overline{Z} \approx \mu\overline{X}$ (figure 6) takes the underlying form

$$P = \overline{X}^{2/3}(Ep_0 + \text{c.c.}) + \cdots + \overline{X}^{-2/3}p_{\text{m}} + \cdots, \tag{3.12}$$

for the pressure, with corresponding expansions for the velocities. The direction factor $\mu = 8^{-1/2}$, while $\overline{Z} - \mu\overline{X} = \overline{X}^{-1/3}\eta$, and the dominant fluctuating part (subscript zero) at this stage has $E = \exp[\mathrm{i}(b_1\overline{X}^2 + \lambda\overline{X}^{2/3}\eta)]$, where $b_1 = 3^{3/2}/16$, $\lambda = (3/8)^{1/2}$ and $\eta \sim 1$. The subscript m refers to the real mean-flow corrections, and c.c. denotes the complex conjugate. The arrangement of the powers of E is partly due to the nonlinear effects and partly to the wave-like dependence in E. The nonlinear interaction is dominated by interplay between the fundamental fluctuations $E^{\pm 1}$ and the mean-flow correction E^0. The strength of this interplay is due physically to the relative slowness of the mean-flow variations; a similar phenomenon also arises in § 3 *b*.

In the present stage the governing equations of concern (Smith *et al.* 1994) are found to be

$$(p_0'' - \eta p_0)' = \mathrm{i}A_{\text{m}}p_0, \tag{3.13}$$

$$-|p_0|^2 = \frac{1}{\pi}\int_{-\infty}^{\infty}\frac{A_{\text{m}}'(q)\,\mathrm{d}q}{(\eta - q)}, \tag{3.14}$$

in normalized form, controlling the complex wave part p_0 and the mean part A_{m}, with $|p_0|$ tending to zero at large $|\eta|$. Here (3.14) stems from a combination of the outer interaction law for the mean-flow components A_{m}, p_{m} and the relation $p_{\text{m}} \propto -|p_0|^2$ obtained from the mean components of the two momentum equations, while (3.13) represents modulation of the wave amplitudes due to the mean-flow (vortex) correction. The critical layer and wall layer also present merely play a secondary role, the former mainly because of the high input amplitude. At lower amplitudes, (3.13) reduces to Airy's equation, in line with earlier theory. At $O(1)$ amplitudes the fast-fluctuation/slow-mean-flow nonlinear mechanism becomes fully active, and computations of the nonlinear system are necessary, sample solutions being presented in the last reference.

At relatively high amplitudes a novel structure is found to emerge. When $|A_{\text{m}}|$ becomes large, the typical scale Δ of $|\eta|$ expands (with $|A_{\text{m}}| \sim \Delta^{3/2}$), and $|p_0|$ also grows, like $\Delta^{1/4}$, yielding the system

$$h^3 + \widetilde{\eta}h = -a_{\text{m}}, \tag{3.15}$$

$$(3h^2 + \widetilde{\eta})r' + (3hh' + 1)r = 0, \tag{3.16}$$

$$-r^2 = \frac{1}{\pi}\int_{-\infty}^{\infty}\frac{a_{\text{m}}'(q)\,\mathrm{d}q}{(\widetilde{\eta} - q)}. \tag{3.17}$$

Here $p_0 \sim \Delta^{1/4}r\exp[\mathrm{i}\Delta^{3/2}f + O(1)]$ and $A_{\text{m}} \sim \Delta^{3/2}a_{\text{m}}$ with the amplitude r, the phase f and the mean part a_{m} all being generally $O(1)$ real functions of the new $O(1)$ coordinate $\widetilde{\eta} \equiv \Delta^{-1}\eta$, and $h \equiv \mathrm{d}f/\mathrm{d}\widetilde{\eta}$. The increasing variation in phase is especially noteworthy. A numerical solution is given in the last reference. At these

PHILOSOPHICAL TRANSACTIONS OF THE ROYAL SOCIETY A MATHEMATICAL, PHYSICAL & ENGINEERING SCIENCES

amplitudes the mean-flow correction comprises relatively long vortices such that the mean displacement increment is mostly positive, except outside the spot where it is negative. The large-Δ theory points to the next interactive structure at an increased amplitude level.

(*b*) *Amplitude level II*

Significant changes occur first when the amplitudes increase slightly to the stage where $\overline{Z}-\mu\overline{X}$ becomes of order unity, corresponding to Δ above rising to the order $\overline{X}^{1/3}$, which yields estimates for the new orders involved. The expansions now holding have $\overline{Z}-\mu\overline{X}=\widehat{\eta}$ being of $O(1)$, and

$$P=\overline{X}^{3/4}(\widehat{E}\widehat{p}_0+\text{c.c.})+\cdots+\overline{X}^{-1/2}\widehat{p}_{\text{m}}+\cdots. \tag{3.18}$$

The primary fluctuating part (here the unknown function $\widehat{f}(\widehat{\eta})$), because of the enhanced phase variation, is $\widehat{E}=\exp[\text{i}(b_1\overline{X}^2+\lambda\overline{X}\widehat{\eta}+\overline{X}^{1/2}\widehat{f}(\widehat{\eta}))]$. The main new contributions at this level come from extra inertial effects in the momentum balances for the mean-flow correction, thus preserving the dominance of the long/short interaction between the fundamental fluctuations and the mean flow. The new controlling equations have the normalized form

$$\widehat{f}'^3+2\widehat{\eta}\widehat{f}'-\widehat{f}=\widehat{A}_{\text{m}}, \tag{3.19}$$

$$(\widehat{\eta}+\tfrac{3}{2}\widehat{f}'^2)(|\widehat{p}_0|)'+(\tfrac{1}{4}+\tfrac{3}{2}\widehat{f}'\widehat{f}''')(\widehat{p}_0)=0, \tag{3.20}$$

$$-\frac{1}{2}\widehat{A}_{\text{m}}-\widehat{\eta}\widehat{A}'_{\text{m}}-(|\widehat{p}_0|^2)'=\frac{1}{\pi}\int_{-\infty}^{\infty}\frac{\widehat{A}''_{\text{m}}(\widehat{q})\,\text{d}\widehat{q}}{(\widehat{\eta}-\widehat{q})}. \tag{3.21}$$

Solutions are presented by Dodia *et al.* (1995). For sufficiently enhanced amplitudes II, the influence of the integral contribution dies out, signalling a diminution of the mean-flow effect produced by the motion near the external stream. Thus, (3.21) reduces to

$$-\tfrac{1}{2}\widehat{A}_{\text{m}}-\widehat{\eta}\widehat{A}'_{\text{m}}=(|\widehat{p}_0|^2)', \tag{3.22}$$

representing a balance between the mean-flow momentum near the wall and the Reynolds-stress effects there due to the amplitude-squared inertia from the main fluctuations. A new stage arising as the amplitude level continues to increase then occurs, when the whole of the trailing-edge region becomes affected by nonlinearity, as the typical $\overline{Z}-\mu\overline{X}$ value rises to $O(\overline{X})$, corresponding to $\widehat{\eta}$ increasing dramatically to $O(\overline{X})$ in effect. Then the mean-flow correction formally becomes comparable with the basic mean flow. In consequence, a strongly nonlinear effect is implied at that level, as investigated below.

(*c*) *Amplitude level III, affecting the entire trailing-edge*

Here the characteristic amplitude level for both the fluctuating and the mean-flow parts is raised to $O(\overline{X})$, in the velocities U,W, with corresponding increases in V,P, as inferred from the previous level (see also figure 6). The nonlinear interactions present now become *strongly nonlinear* however, and, effectively, all the higher harmonic fluctuations also play a significant role. Since $\overline{Z}$- and $\overline{X}$-variations are comparable when the whole of the trailing-edge region is considered, we work in terms of the polars R,θ, where $(\overline{X},\overline{Z})=R(\cos\theta,\sin\theta)$, and now θ is $O(1)$ typically,

with R being large. Hence the flowfield solution has

$$\overline{U} = R(\overline{U}_{\rm m} + \overline{U}_{\rm f}) + \cdots, \quad \overline{W} = R(\overline{W}_{\rm m} + \overline{W}_{\rm f}) + \cdots, \quad P = R^2\overline{P}_{\rm f} + (\overline{P}_{\rm m} + P_{\rm f}) + \cdots, \tag{3.23}$$

where $\overline{U}, \overline{W}$ are the R- and θ-velocities, respectively. In the above equations, the subscripts m, f refer to the mean and fluctuating parts, respectively, the latter having zero mean. The *total* mean flow, e.g. $\overline{U}_{\rm m}$, is unknown now but it varies slowly, being dependent on $\overline{Y}, \theta$, whereas the unknown fluctuations, e.g. $\overline{U}_{\rm f}$, also depend on the rapid variable $F \equiv b(\theta)R^2$. Smith *et al.* (1994) show that a closed nonlinear system is produced controlling the major unknowns, namely the dominant fluctuations, the total mean flow, and the phase function $b(\theta)$.

(*d*) *The spot centre*

In the main body of the spot, at larger distances $x \sim t$ downstream, the full Euler equations (3.1) ff. come back into play, from the following reasoning. Formally, the scaled distances $\overline{X}, \overline{Z}$, and hence R, then tend to $O(t^{1/2})$, to make x, z be of order t. It follows that the y-scale that was originally $t^{-1/2}$ in the lowest layer of (3.8), but was then enhanced by a factor $O(R)$ in § 3 *a–c* above, rises to $O(1)$. Simultaneously, the uppermost y-scale behaves as $t^{1/2}R^{-1}$ typically because of the fast $E, \widehat{E}$ or F variations in § 3 *a–c* above, and so it also tends to $O(1)$ as R increases to the order $t^{1/2}$, while the y-scale of the middle layer in (3.9) stays $O(1)$. Therefore, the three-layer structure collapses now into a single structure. Along with this, the characteristic variation of the fluctuating parts, with respect to x, z, now becomes faster due to the rapid F (or $E, \widehat{E}$) dependence, essentially by a length factor of order R^{-1}, or $t^{-1/2}$; derivatives involving F are greater than those not involving F by a factor $O(R^2)$. This implies that the characteristic length scale in x, z falls to $O(1)$ as far as the fluctuations are concerned. Again, the strong nonlinearity encountered in § 3 *c* points to strong nonlinearity persisting as the $x = O(t)$ zone is encountered downstream. For example, the velocity u then becomes $O(1)$, from § 3 *a–c*. All the above then leads to the full unsteady 3D Euler system, holding in the centre of the spot, and implying a large numerical task. That is, however, not the whole story. For, according to § 3 *c*, there is significant interplay between those fast fluctuations and the more slowly varying total mean flow. So there must be extra length scales in operation, specifically lengths x, z of $O(t)$ (from reasoning as in the previous paragraph), in addition to the $O(1)$ length scales above. The extra length scales are associated predominantly with the equations (slender-flow equations) for the mean flow and must play an equally important role, linking the main short- and long-scale behaviour in similar fashion to the links in § 3 *c*.

Moreover, as the spot continues even further downstream, to distances x, z of order $Re^{1/2}$ measured from the initial disturbance, i.e. global distances, $\overline{x}, \overline{z}$ of $O(1)$, since $(\overline{x}, \overline{z}) = Re^{-1/2}(x, z)$, the two interacting short- and long-length scales above become $O(Re^{-1/2})$ and $O(1)$ respectively, in the global coordinates $\bar{x}, \bar{z}$, with the normal coordinate staying at $O(Re^{-1/2})$. These scalings appear to be physically sensible. A new feature arises, however, since viscous forces must affect the mean-flow equations on the $\bar{x}, \bar{z} \sim 1$ scale. Indeed, the 3D boundary-layer equations are implied,

$$\bar{u}_{\bar{x}} + \bar{v}_y + \bar{w}_{\bar{z}} = 0, \tag{3.24}$$

$$\bar{u}_{\bar{t}} + \bar{u}\bar{u}_{\bar{x}} + \bar{v}\bar{u}_y + \bar{w}\bar{u}_{\bar{z}} = \bar{s}_1 - \bar{p}_{\bar{x}} + \bar{u}_{yy}, \tag{3.25}$$

$$\bar{w}_{\bar{t}} + \bar{u}\bar{w}_{\bar{x}} + \bar{v}\bar{w}_y + \bar{w}\bar{w}_{\bar{z}} = \bar{s}_2 - \bar{p}_{\bar{z}} + \bar{w}_{yy}, \tag{3.26}$$

PHILOSOPHICAL TRANSACTIONS OF THE ROYAL SOCIETY A MATHEMATICAL, PHYSICAL & ENGINEERING SCIENCES

essentially for the unknown mean-flow velocities $(\bar{u}, \bar{v}, \bar{w})(\bar{x}, y, \bar{z}, \bar{t})$, where $\bar{t} \equiv Re^{-1/2}\, t$ denotes the global time. Here $\bar{p}(\bar{x}, \bar{z}, \bar{t})$ is the prescribed external-stream pressure, associated with $(\bar{u}, \bar{w}) \to (u_e, w_e)(\bar{x}, \bar{z}, \bar{t})$ say, as $y \to \infty$, whereas $\bar{s}_1, \bar{s}_2$ are the unknown Reynolds stress terms comprising nonlinear effects from the fluctuating velocity components governed by (3.1)–(3.7). The full interaction between (3.24)–(3.26) and (3.1)–(3.7) also involves the mean profile $\bar{u} = u_B$ in (3.6), which is now dependent on $\bar{x}, y, \bar{z}, \bar{t}$ and unknown, as is the corresponding non-zero $\bar{w} = w_B$ in general. It is intriguing that, according to the above argument, the flow properties on those two length scales remain fully interactive, with the viscous 3D boundary-layer system (3.24)–(3.26) and the inviscid 3D Euler system (3.1)–(3.7) being coupled together via the Reynolds stresses in (3.25), (3.26) and the profiles in (3.6). See figure 4 of Smith *et al.* (1994) and figure 6 here, and observe that interference is assumed to be negligible from the elliptic $O(Re^{-1/4})$ zone that was originally the $O(t^{1/2})$ zone, lying behind the spot and surrounding the initial station.

As with other aspects, the present area seems to merit much further research. The impact of high-amplitude analysis, for example, remains to be studied here. In addition to the above broader-scale behaviour, however, there are finer-scale responses to consider, as in the following subsection.

(*e*) *Internal dynamics and viscous effects*

The major element missing so far in § 3 is viscosity, which substantially governs the finer-scale dynamics and the connection with larger scales, apart from the interesting global-scale effect predicted in (3.24) ff. Although our concern in the majority of § 3 is with global features, we also consider the internal features briefly below, more details and description being given in § 2 and in the references cited therein.

An important role is played by the 3D viscous sublayer or sublayers lying (initially) between the mainly inviscid regions of § 3 *a*–*c* and the solid surface. The sublayer is neglected above, as it is assumed to remain relatively thin; and that seems likely to stay true for the first stages I, II. At higher amplitudes such as III however, the sublayer, which initially occupies only a small fraction $O(Re^{-1/4})$ of the complete boundary layer, is governed by the classical non-interactive unsteady 3D boundary-layer formulation ((3.24)–(3.26) in effect, without the Reynolds-stress terms) holding beneath the Euler form of (3.1) ff. Hence, the sublayer is subjected to strong unsteady pressure gradients, including adverse ones, produced, for instance, by the strongly nonlinear inviscid behaviour in III. First thoughts would suggest (figure 6) that, under such prescribed pressure gradients, the sublayer erupts in the sense of its solution becoming singular within a finite time in the Van Dommelen (1981) fashion, such that

$$\delta_1 \to \infty, \quad \text{as } t \to t_1 - . \tag{3.27}$$

Here δ_1 is the usual scaled sublayer displacement thickness, the singular time t_1 is finite, and (3.27) occurs locally at a particular x station; see the structure involved in Elliott *et al.* (1983). The singularity is especially relevant if the inviscid Euler behaviour predicted by § 3 *c* or (3.1)–(3.7) becomes extreme in its amplitude variation. Again, (3.27) is written as if for 2D flow but the 3D case appears predominantly quasi-2D anyway (Elliott *et al.* 1983; Cowley *et al.* 1991). More significantly, the flow solution next moves into shorter length and time scales until inner–outer interaction takes place between the increasing displacement (effectively δ_1) and the induced pressure due to back-influence from the inviscid slip stream outside, as described by Elliott *et al.* (1983). At that stage the work of Brown *et al.* (1988) comes into play,

implying a further and stronger singularity in the displacement as well as in the local pressure, and hence yet newer physics enters the reckoning. Recent theoretical and computational studies of that stage have been made by Cassel *et al.* (1995), with the present author extending the work.

Further thought however points to the finite-time breakup of § 2 being more likely to arise in practical as well as theoretical terms, depending on the precise context. This nonlinear breakup singularity is associated with inner–outer *interaction* affecting the sublayer and such interaction is always present. The breakup occurs at a time (t_2 say) earlier than the non-interactive time t_1 above, since the nonlinear breakup criterion (2.13) is met earlier. See Cassel *et al.* (1995). The breakup involves the local response

$$|\partial p/\partial x| \to \infty, \quad \tau_w \to \infty, \quad \text{as } t \to t_2 - \tag{3.28}$$

in particular (see § 2), with the pressure remaining finite but the pressure gradient and the normalized wall shear stress τ_w becoming infinite in anticipation of a change of scale. The breakup in (3.28) is followed by the entry of new physical effects locally, as described in § 2.

4. Further comments

There is still much to be explained. Following on directly from § 3, finite-time breakups must occur sooner or later, and further work is needed to understand the impact of these internal eruptive or bursting processes on the larger-scale evolution addressed in § 3, and the generation of faster time and length scales and hence higher frequency and wavenumber spectral content. There is in particular the issue of whether or not a clear link can be established between the formation of hairpin vortices in reality, the observed hierarchy of scales, and the so-called turbulence reproduction cycle (see 'domino process' earlier) near the surface (see, for example, Smith C. R. *et al.* 1991; Grass *et al.* 1991). Certainly, viscous-induced eruptions as in (3.27), (3.28) can also take place in other scales, both larger as in the context of (3.24)–(3.26) and smaller, cf. the cascade process described by Smith *et al.* (1990), which predicts the scales

$$O(Re^{-1} \ln Re), \tag{4.1}$$

$$O(Re^{-3/4}), \tag{4.2}$$

for the final turbulent sublayer thickness and the microscale of the mid-flow, respectively, in agreement with common turbulence models and the Kolmogorov estimate.

The research on spots is felt to be in an interesting and challenging state as regards both the global and the internal properties considered theoretically above for nonlinear spots. The strong more global nonlinearity encountered in § 3 *c*,*d* is particularly exciting, as is that in § 3 *e* and § 2 for the more internal flow features and spikes. We would especially highlight the novel interaction that arises on the largest scale (airfoil scale), as covered by (3.24)–(3.26) coupled with (3.1)–(3.7). However, the highest amplitudes tackled so far, in § 3 *c*,*d*, require concerted further study. A related point is that markedly different flow structures might be set up sufficiently far downstream of the initial disturbance with different scales acting as mentioned in § 1, although there is little work in connecting these structures with an initial-value 3D problem as here. Our stress here is towards full nonlinearity, but much other work is desirable on linear or weakly nonlinear problems, on properties near the spot leading edge (cf. Bowles & Smith 1995), and on compressibility effects, given Clark *et al.*'s

PHILOSOPHICAL TRANSACTIONS OF THE ROYAL SOCIETY A MATHEMATICAL, PHYSICAL & ENGINEERING SCIENCES

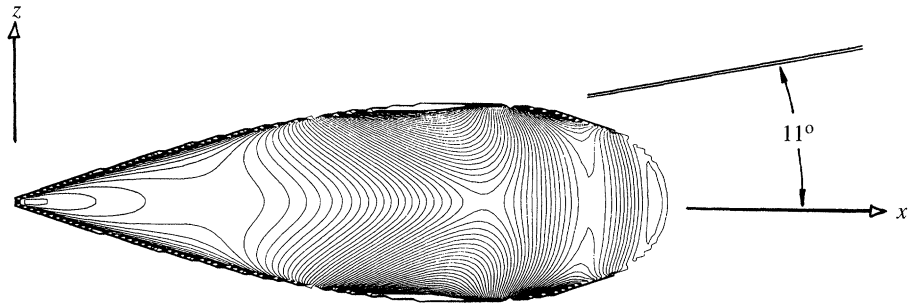

Figure 7. Theoretical spot solution from Bowles & Smith (1994) incorporating short-scale effects, and comparison with the typical 11° spread angle found experimentally.

(1994) demonstration of experimental agreement with the Doorly & Smith (1992) theory over a range of Mach numbers; channel flows and wall jets are considered by Dodia (1994). While a wide variety of scales act within the 3D spot evolution identified by theory, agreeing with the description of 'spots within spots', and the overall picture looks fairly encouraging and self-consistent as a basis for continuing study, much remains to be done.

So far, the spot theory tentatively appears to fall in line with all the experimental findings summarized in § 1 in a qualitative or quantitative sense. Although, at first, agreement with experiments seems poor for the spot-spreading rate (in plan view), a recent study by Bowles & Smith (1995) points to important short-scaled effects combined with those of nonlinearity above, to give a theoretical spread angle (figure 7) of approximately 11°, very close to the experimental observations. On more global features (§ 3), tentative agreement with experiments and computations is demonstrated in Smith (1991*a*) for the initial-value problem (3.1) ff. alone, while Bowles & Smith (1995) above suggest quantitative agreement. On the more internal features, quantitative agreement with computations and experiments has been noted in § 2 and is shown in figures 2–5; in particular the breaking point in figure 4 signals the onset of turbulent spots in the forced flow there, linking with the free type of spot considered in § 3. Comparisons of the integral criterion (2.13) with direct numerical simulation results are currently being made (in conjunction with Dr R. I. Bowles, Dr S. P. Fiddes and Dr N. Sandham), in addition to those with experiments in figure 2, which we repeat are at *subcritical* Reynolds numbers, indicating wide application of the theory (see Smith *et al.* 1984). Thus, while there is undoubtedly a vast amount still unknown on the theoretical side, there is now a fair range of quite supportive agreements between rational theory and its interpretations on the one hand and experiments on the other, in deep transition.

Support from EPSRC, U.K., for computing facilities, and from ARO (contract no. DAAL03-92-G-0040) and the United Tech. Independent Research Program, is gratefully acknowledged, as is the interest of Dr R. G. A. Bowles, Dr R. I. Bowles, Dr B. T. Dodia and Professor J. D. A. Walker.

References

Benney, D. J. & Chow, C. 1989 *Stud. appl. Math.* **80**, 37.

Bertolotti, F. P., Herbert, Th. & Spalart, P. R. 1992 *J. Fluid Mech.* **242**, 442–474.

Bowles, R. G. A. & Smith, F. T. 1995 *J. Fluid Mech.* (In the press.)

Bowles, R. I., Smith, F. T. & Walker, J. D. A. 1995 (In preparation.)

Brown, S. N., Cheng, H. K. & Smith, F. T. 1988 *J. Fluid Mech.* **193**, 191–216.

PHILOSOPHICAL TRANSACTIONS OF THE ROYAL SOCIETY A MATHEMATICAL, PHYSICAL & ENGINEERING SCIENCES

Bullister, E. T. & Orszag, S. A. 1987 Numerical simulation of turbulent spots in channel and boundary-layer flows. *J. scient. Comput.* **2**, 263–281.

Cassel, K., Smith, F. T. & Walker, J. D. A. 1995 *J. Fluid Mech.* (Submitted.)

Chambers, F. W. & Thomas, A. S. W. 1983 Turbulent spots, wave packets and growth. *Phys. Fluids* **26**, 1160–1162.

Churilov, S. M. & Shukman, I. G. 1987 *J. Fluid Mech.* **180**, 1–20.

Churilov, S. M. & Shukman, I. G. 1988 *J. Fluid Mech.* **194**, 187–216.

Clark, J. P., Jones, T. V. & LeGraff, J. E. 1994 *J. engng Math.* **28**, 1–19.

Cohen, J., Breuer, K. S, & Haritonidis, J. H. 1991 On the evolution of a wave packet in a laminar boundary layer. *J. Fluid Mech.* **225**, 575–606.

Conlisk, A. T., Burggraf, O. R. & Smith, F. T. 1987 Nonlinear neutral modes in the Blasius boundary layer. In *Transactions of the ASME. Forum on unsteady separation.* Cincinnati, Ohio, June 1987.

Cowley, S. J., van Dommelen, L. L. & Lam, S. T. 1991 On the use of Lagrangian variables in descriptions of unsteady boundary-layer separation *Phil. Trans. R. Soc. Lond.* A **333**, 343–378.

Dodia, B. T., Bowles, R. G. A. & Smith, F. T. 1995 *J. engng Math.* (Submitted.)

Dodia, B. T. 1994 Ph.D. thesis, University of London.

Doorly, D. J. & Smith, F. T. 1992 Initial-value problems for spot disturbances in incompressible or compressible boundary layers. *J. engng Math.* **26**, 87–106.

Duck, P. W. 1985 Laminar flow over unsteady humps: the formation of waves. *J. Fluid Mech.* **160**, 465–498.

Elliott, J. W., Cowley, S. J. & Smith, F. T. 1983 Breakdown of boundary layers: (i) on moving surfaces, (ii) in semi–similar unsteady flow; (iii) in fully unsteady flow. *Geophys. Astrophys. Fluid Dyn.* **25**, 77–138.

Emmons, H. W. 1951 The laminar-turbulent transition in a boundary layer, Part 1. *J. aeronaut. Sci.* **18**, 490–498 (see also 1963 *J. Fluid Mech.* **9**, 235–246).

Falco, R. E. 1979 Structural aspects of turbulence in boundary layer flows. In *Proc. 6th Biennial Symp. Turb.* (ed. J. K. Zakin & G. K. Patterson), ch. 1.1–1.4. University of Missouri-Rolla.

Fasel, H. 1984 Numerical investigations of two-dimensional development in boundary-layer transition. In *Proc. Symp. on Turbulent and Chaotic Phenomena in Fluids* (ed. T. Tatsumi), pp. 94–103. New York: Elsevier.

Fasel, H. 1990 Numerical solution of instability and transition in boundary-layer flows. In *Laminar-turbulent transition* (ed. D. Arnal & R. Michel). Berlin: Springer.

Gad-el-Hak, M., Blackwelder, R. F. & Riley, J. J. 1981 On the growth of turbulent regions in laminar boundary layers. *J. Fluid Mech.* **110**, 73–95.

Gaster, M., 1968, The development of three-dimensional wave packets in a boundary layer. *J. Fluid Mech.* **32**, 172–184.

Goldstein, M. E. 1985 Scattering of acoustic waves into Tollmien–Schlichting waves by small streamwise variations in surface geometry. *J. Fluid Mech.* **154**, 509–530.

Goldstein, M. E. & Hultgren, L. S. 1989 Boundary-layer receptivity to long-wave freestream disturbances. *Ann. Rev. Fluid Mech.* **21**, 137–166.

Grass, A. J., Stuart, R. J. & Mansour-Tehrani, M. 1991 Vortical structures and coherent motion in turbulent flow over smooth and rough boundaries. *Phil. Trans. R. Soc. Lond.* A **336**, 35–65.

Hall, P. & Smith, F. T. 1984 *Stud. appl. Math.* **70**, 91–120.

Hall, P. & Smith, F. T. 1988 *Proc. R. Soc. Lond.* A **417**, 255–282.

Hall, P. & Smith, F. T. 1989 *Eur. J. Mech.* B **8**, 179–205.

Hall, P. & Smith, F. T. 1990 *Instability and transition II* (ed. M. Y. Hussaini & R. G. Voigt). Berlin: Springer.

PHILOSOPHICAL TRANSACTIONS OF THE ROYAL SOCIETY A MATHEMATICAL, PHYSICAL & ENGINEERING SCIENCES

Hall, P. & Smith, F. T. 1991 On strongly nonlinear vortex-wave interactions in boundary layer transition. *J. Fluid Mech.* **227**, 641–666 (see also 1989 Report, Institute for Computer Applications in Science and Engineering. pp. 89–92).

Head, M. R. & Bandyopadhay, P. 1981 New aspects of turbulent boundary-layer structure. *J. Fluid Mech.* **107**, 297–338.

Henningson, D. S. & Alfredson, P. H. 1987 The wave structure of turbulent spots in a plane Poiseuille flow. *J. Fluid Mech.* **178**, 405–421.

Henningson, D. S., Spalart, P. R. & Kim, J. 1987 Numerical simulations of turbulent spots in plane Poiseuille and boundary-layer flow. *Phyics Fluids.* **30**, 2914–2917.

Henningson, D. S. & Kim, J. 1991 On turbulent spots in a plane Poiseuille flow. *J. Fluid Mech.* **228**, 183–205.

Hoyle, J. M., Smith, F. T. & Walker, J. D. A. 1991 On sublayer eruption and vortex formation. *Comp. Phys. Comms.* **65**, 151–157 (see also Hoyle, J. M. 1992 Ph.D. thesis, University of London).

Hoyle, J. M. & Smith, F. T. 1994 *Proc. R. Soc. Lond.* A **447**, 467–492.

Johannson, A. V., Her, J. & Haritonidis, J. H. 1987 On the generation of high-amplitude wall-pressure peaks in turbulent boundary-layers and spots. *J. Fluid Mech.* **175**, 119–142.

Kachanov, Y. S., Ryzhov, O. S. & Smith, F. T. 1993 Formation of solitons in transitional boundary layers: theory and experiment. *J. Fluid Mech.* **251**, 273–297.

Katz, T., Seifert, A. & Wygnanski, I. J. 1990 On the evolution of the turbulent spot in a laminar boundary layer with a favourable pressure gradient. *J. Fluid Mech.* **221**, 1–22.

Klebanoff, P. S. & Tidstrom, K. D. 1959 The evolution of amplified waves leading to transition in a boundary layer with zero pressure gradient. *NASA tech. Note* D–195 (see also 1963 Stuart, J. T. *Laminar boundary layers* (ed. L. Rosenhead), ch. IX. Oxford University Press).

Konzelmann, U. & Fasel, H. 1991 Numerical simulation of a three-dimensional wave packet in a growing flat plate boundary layer. In *Proc. R. Aero. Soc. Meeting on Transition*, Cambridge, UK.

Leonard, A. 1981 *Turbulent structures in wall-bounded shear flow observed via three-dimensional numerical simulations.* Springer Lecture Notes in Physics, vol. 136, pp. 119–145. Berlin: Springer.

Lighthill, M. J. 1963 *Introduction to boundary layer theory. Laminar boundary layers* (ed. L. Rosenhead), ch. II. Oxford University Press.

Lundbladh, A. & Johansson, A. V. 1991 Direct simulation of turbulent spots in plane Couette flow. *J. Fluid Mech.* **229**, 499–516.

Nishioka, M., Asai, M. & Iida, S. 1979 An experimental investigation of the secondary instability. In *Laminar-turbulent transition.* Berlin: Springer.

Peridier, V. J., Smith, F. T. & Walker, J. D. A. 1991*a* Vortex-induced boundary-layer separation. Part 1. The unsteady limit problem $Re \rightarrow \infty$. *J. Fluid Mech.* **232**, 99–131.

Peridier, V. J., Smith, F. T. & Walker, J. D. A. 1991*b* Vortex-induced boundary-layer separation. Part 2. Unsteady interacting boundary layer theory. *J. Fluid Mech.* **232**, 132–165.

Perry, A. E., Liu, T. T. & Teh, E. W. 1981 A visual study of turbulent flows. *J. Fluid Mech.* **104**, 387–405.

Robinson, S. K. 1991 Coherent motions in the turbulent boundary layer. *Ann. Rev. Fluid Mech.* **23**, 601–639.

Ruban, A. I. 1985 On the generation of Tollmien–Schlichting waves by sound. *Fluid Dyns.***19**, 709–716.

Savenkov, I. V. 1993 *J. Fluid Mech.* **252**, 1–30.

Schlichting, H. 1979 *Boundary-layer theory*, 4th edn. New York: McGraw-Hill.

Schubauer, G.B. & Klebanoff, P.S., 1956, Contributions on the mechanics of boundary layer transition. NACA Rep. 1289.

Smith, F. T. 1979*a* *Proc. R. Soc. Lond.* A **366**, 91–109.

PHILOSOPHICAL TRANSACTIONS OF THE ROYAL SOCIETY A MATHEMATICAL, PHYSICAL & ENGINEERING SCIENCES

Smith, F. T. 1979*b* Nonlinear stability of boundary layers for disturbances of various sizes. *Proc. R. Soc. Lond.* A **368**, 573–589.

Smith, F. T. 1984 *AIAA Jl* 84–1582 (see also 1985 Utd. Tech. Res. Cent. Rept. UTRC85–36, Hartford, CT).

Smith, F. T. 1987 Breakup in unsteady separation. In *Trans. of the ASME Conf. on Unsteady Separation*, Cincinnati, OH.

Smith, F. T. 1988*a* Finite-time breakup can occur in any unsteady interacting boundary layer. *Mathematika* **35**, 256–273.

Smith, F. T. 1988*b* A reversed-flow singularity in interacting boundary layers. *Proc. R. Soc. Lond.* A **420**, 21–52.

Smith, F. T. 1991*a* Steady and unsteady 3D interactive boundary layers. *Comp. Fluids* **20**, 243–168 (Also given as a presentation at the R. T. Davis Memorial Symp., Cincinnati, USA 1987).

Smith, F. T. 1991*b* Composite, Navier–Stokes and Euler unsteady-flow computations in boundary layers. *Utd. Tech. Res. Cent. Rept.* UTRC91–2, Hartford, CT.

Smith, F. T. 1992 On nonlinear effects near the wing-tips of an evolving boundary-layer spot. *Phil. Trans. R. Soc. Lond.* A **340**, 131–165.

Smith, F. T. & Bowles, R. I. 1992 Transition theory and experimental comparisons on (I) amplification into streets and (II) a strongly nonlinear breakup criterion. *Proc. R. Soc. Lond.* A **439**, 163–175.

Smith, F. T., Brown, P. G. & Brown, S. N. 1993 Initiation of three-dimensional nonlinear transition paths from an inflexional profile. *Eur. J. Mech.* **12**, 447–473.

Smith, F. T. & Burggraf, O. R. 1985 On the development of large-sized short-scaled disturbances in boundary layers. *Proc. R. Soc. Lond.* A **399**, 25–255.

Smith, F. T., Dodia, B. T. & Bowles, R. G. A. 1994 *J. engng Math.* **28**, 73–91.

Smith, F. T., Doorly, D. J. & Rothmayer, A. P. 1990 On displacement thickness, wall-layer and mid-flow scales in turbulent boundary layers, and slugs of vorticity in pipes and channels. *Proc. R. Soc. Lond.* A **428**, 255–281.

Smith, F. T., Papageorgiou, D. T. & Elliott, J. W. 1984 An alternative approach to linear and nonlinear stability calculations at finite Reynolds numbers. *J. Fluid Mech.* **146**, 313–330.

Smith, C. R., Walker, J. D. A., Haidari, A. H. & Sobrun, U. 1991 On the dynamics of near-wall turbulence. *Phil. Trans. R. Soc. Lond.* A **336**, 131–175.

Smith, F. T. & Walton, A. G. 1989 Nonlinear interaction of near-planar TS waves and longitudinal vortices in boundary-layer transition. *Mathematika* **36**, 262–289.

Stewart, P. A. & Smith, F. T. 1992 Three-dimensional nonlinear blow-up from a nearly planar initial disturbance, in boundary-layer transition: theory and experimental comparisons. *J. Fluid Mech.* **244**, 79–100.

Stuart, J. T. 1963 *Laminar boundary layers* (ed. L. Rosenhead), ch. IX. Oxford University Press.

Timoshin, S. N. & Smith, F. T. 1995 *J. Fluid Mech.* (Submitted.)

Van Dommelen, L. L. 1981 Unsteady boundary-layer separation. Ph.D. thesis, University of Cornell.

Vickers, I. P. & Smith, F. T. 1994 *J. Fluid Mech.* **268**, 147–173.

Walker, J. D. A. 1990 Wall-layer eruptions in turbulent flows. In *Proc. 2nd IUTAM Symp. on structure of turbulence and drag reduction* (ed. A. Gyr), pp. 109–117. New York: Springer.

Walton, A. G. & Smith, F. T. 1992 Properties of strongly nonlinear vortex/Tollmien–Schlichting waves interactions. *J. Fluid Mech.* **244**, 649–676.

Walton, A. G., Bowles, R. I. & Smith, F. T. 1994 *Eur. J. Mech.* B **13**, 629–655.

Wu, X. 1993 *J. Fluid Mech.* **256**, 685–719.

Zhuk, V. I. & Ryzhov, O. S. 1982 *Soviet. Phys. Dokl.* **27**, 177–179.

PHILOSOPHICAL TRANSACTIONS OF THE ROYAL SOCIETY A MATHEMATICAL, PHYSICAL & ENGINEERING SCIENCES